The Addition Reaction between Silylene and Ethyne: Further Isotope Studies, Pressure Dependence Studies, and Quantum Chemical Calculations

Rosa Becerra,[†] J. Pat Cannady,[‡] Guy Dormer,[§] and Robin Walsh*[,§]

Instituto de Quimica-Fisica 'Rocasolano', C.S.I.C., C/Serrano 119, 28006 Madrid, Spain, Dow Corning Corporation, P.O. Box 994, Mail CO11232, Midland, Michigan, 48686-0994, and Department of Chemistry, University of Reading, Whiteknights, P.O. Box 224, Reading, RG6 6AD, U.K.

Received: April 18, 2008; Revised Manuscript Received: June 20, 2008

Time-resolved kinetic studies of the reaction of dideutero-silylene, SiD_2, generated by laser flash photolysis of phenylsilane-d_3, have been carried out to obtain rate constants for its bimolecular reaction with C_2H_2. The reaction was studied in the gas phase over the pressure range 1−100 Torr in SF_6 bath gas, at five temperatures in the range 297−600 K. The second-order rate constants obtained by extrapolation to the high-pressure limits at each temperature fitted the Arrhenius equation $\log(k^{\infty}/\mathrm{cm^3\ molecule^{-1}\ s^{-1}}) = (-10.05 \pm 0.05) + (3.43 \pm 0.36\ \mathrm{kJ\ mol^{-1}})/RT\ \ln 10$. The rate constants were used to obtain a comprehensive set of isotope effects by comparison with earlier obtained rate constants for the reactions of SiH_2 with C_2H_2 and C_2D_2. Additionally, pressure-dependent rate constants for the reaction of SiH_2 with C_2H_2 in the presence of He (1−100 Torr) were obtained at 300, 399, and 613 K. Quantum chemical (ab initio) calculations of the SiC_2H_4 reaction system at the G3 level support the initial formation of silirene, which rapidly isomerizes to ethynylsilane as the major pathway. Reversible formation of vinylsilylene is also an important process. The calculations also indicate the involvement of several other intermediates, not previously suggested in the mechanism. RRKM calculations are in semiquantitative agreement with the pressure dependences and isotope effects suggested by the ab initio calculations, but residual discrepancies suggest the possible involvement of the minor reaction channel, $SiH_2 + C_2H_2 \rightarrow Si(^3P_1) + C_2H_4$. The results are compared and contrasted with previous studies of this reaction system.

Introduction

Silylene, SiH_2, is the prototype heavy carbene and is of particular importance because of its involvement in the thermal and photochemical breakdown mechanisms of silicon hydrides and organosilanes, as well as being a key intermediate in CVD. Time-resolved kinetic studies, carried out in recent years, have shown that it reacts rapidly and efficiently with many chemical species.[1−3] Examples of its reactions include Si−H bond insertions, C=C and C≡C π-bond additions.[4] This paper concerns the prototype addition reaction with ethyne. Previous kinetic studies, by two of us,[5] have shown that the reaction is a pressure dependent association process, with the rate approaching the collisional limit at high pressures. However, RRKM modeling of the pressure dependence was not consistent with the formation of the simple silacycle, silirene, as the single product, based on the energy requirement of the calculation. This led to the hypothesis that some of the silirene was isomerized to ethynylsilane (silylacetylene). Further studies[5,6] of the isotopic variant system, $SiH_2 + C_2D_2$, revealed a large inverse kinetic isotope effect which was pressure dependent. This suggested that there is a further reaction pathway involving the formation of vinylsilylene from silirene, which can effectively scramble the H and D labels and thereby provide further, nonpressure-dependent pathways. The mechanism is summarized in Scheme 1.

SCHEME 1

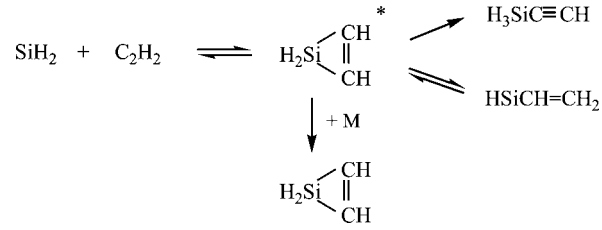

Although this scheme seems to contain the essential steps required to fit the observed kinetics and was broadly consistent with the energetics of the species involved (estimated mainly by the methods of thermochemical kinetics[7]), it is now possible to augment these by a fuller exploration of the potential energy surface. Published quantum chemical studies of this reaction system[8−14] are in broad agreement with the mechanism of Scheme 1 but have not considered some other plausible reaction intermediates. An additional motivation for the present study was an earlier investigation, involving two of us,[15] of the apparently analogous reaction of $GeH_2 + C_2H_2$. The kinetics of this latter reaction showed virtually no pressure dependence, and the explanation for this, supported by quantum chemical (ab initio) calculations, was the occurrence of the process:

$$GeH_2 + C_2H_2 \rightarrow Ge(^3P_1) + C_2H_4$$

The counterpart of this process in the $SiH_2 + C_2H_2$ reaction, viz. Si atom formation, was not previously invoked, because the observed pressure dependences appeared to require an association reaction. Nevertheless, its potential involvement

* E-mail: r.walsh@reading.ac.uk.
[†] Instituto de Quimica-Fisica 'Rocasolano'.
[‡] Dow Corning Corporation.
[§] University of Reading.

10.1021/jp803391g CCC: $40.75 © 2008 American Chemical Society
Published on Web 08/21/2008

needs to be considered. It is also possible to extend the isotope and pressure-dependence studies to provide further experimental evidence to assist the unravelling of this complex mechanism. Thus, we present here (i) new quantum chemical calculations of the potential energy surface, (ii) an extension of the pressure-dependence studies of $SiH_2 + C_2H_2$, this time in the presence of a weak collision partner, helium, more likely to show up mechanistic anomalies at low pressures than SF_6, previously used, (iii) kinetic studies of the $SiD_2 + C_2H_2$ reaction, not previously investigated, in order to extend our knowledge of the isotope effects, and (iv) RRKM calculations undertaken to explore the extent to which the new kinetic data can be fitted to the calculated energetics.

For book-keeping purposes, we use the following reaction numbering system:

$$SiH_2 + C_2H_2 \rightarrow \text{products} \quad \text{(H)}$$

$$SiD_2 + C_2H_2 \rightarrow \text{products} \quad \text{(D1)}$$

$$SiH_2 + C_2D_2 \rightarrow \text{products} \quad \text{(D2)}$$

Experimental Section

Equipment, Chemicals, and Method. The apparatus and equipment for these studies have been described in detail previously.[16,17] Only essential and brief details are therefore included here. Silylenes were produced by the 193 nm flash photolysis of appropriate precursors by using a Coherent Compex 100 exciplex laser. The precursor molecules were phenylsilane, $PhSiH_3$ (for SiH_2), and phenylsilane-d_3 ($PhSiD_3$, for SiD_2). Photolysis pulses (beam cross section 4 cm × 1 cm) were fired into a variable -emperature quartz reaction vessel with demountable windows at right angles to its main axis. Silylene (SiH_2, SiD_2) concentrations were monitored in real time by means of a Coherent 699-21 single-mode dye laser pumped by an Innova 90-5 argon ion laser and operating with Rhodamine 6G. The monitoring laser beam was multipassed 36 times along the vessel axis, through the reaction zone, to give an effective path length of 1.5 m. A portion of the monitoring beam was split off before entering the vessel for reference purposes. For SiH_2 detection, the monitoring laser was tuned to 17259.50 cm^{-1}, corresponding to the known $^RQ_{0,J}$ (5) strong rotation transition[18] in the $\tilde{A}^1B_1(0,2,0) \leftarrow \tilde{X}^1A_1(0,0,0)$ vibronic absorption band. For SiD_2 detection, the known (but unassigned) transition at 17387.07 cm^{-1} [19] was used for monitoring. Light signals were measured by a dual photodiode/differential amplifier combination, and signal decays were stored in a transient recorder (Datalab DL910) interfaced to a BBC microcomputer. This was used to average the decays of 5−15 photolysis laser shots (at a repetition rate of 0.5 or 1 Hz). The averaged decay traces were processed by fitting the data to an exponential form by using a nonlinear least-squares package. This analysis provided the values for first-order rate coefficients, k_{obs}, for removal of SiH_2 or SiD_2 in the presence of known partial pressures of substrate gas.

Gas mixtures for photolysis were made up, containing 2.0−6.0 mTorr of precursor (either $PhSiH_3$ or $PhSiD_3$) and 0−530 mTorr of C_2H_2. Inert diluent (SF_6 or He) was also added (up to 100 Torr). [Note: 1Torr = 133.3 N m^{-2}.] Pressures were measured by capacitance manometers (MKS, Baratron). All gases used in this work were frozen and rigorously pumped to remove any residual air prior to use. $PhSiH_3$ (99.9%) was obtained from Ventron-Alfa (Petrarch). $PhSiD_3$ was prepared as previously described[19] and purified to 99.8%. C_2H_2 was obtained from British Oxygen. It was distilled at low temperature (195 K) to remove condensable impurities (CH_3COCH_3) and subsequently found to contain no gas-chromatographically detectable impurities (>99.9%). Sulfur hexafluoride, SF_6 (no GC-detectable impurities), was from Cambrian Gases. Helium, He (no GC-detectable impurities), was from BOC. GC purity checks were carried out with both a 3 m silicone oil column (OV101) operated at 60 °C and a 3 m Porapak Q operated at 120 °C. N_2 was used as carrier, gas and detection was performed by FID. Detection limits for impurity peaks were better than 0.1% of the principal component.

Ab Initio Calculations. The electronic structure calculations were performed with the Gaussian 98 software package.[20] All structures were determined by energy minimization at the MP2=Full/6-31G(d) level. Transition-state structures were characterized as first-order saddle points by calculation of the Hessian matrix. Stable structures, corresponding to energy minima, were identified by possessing no negative eigenvalues of the Hessian, whereas transition states were identified by having one and only one negative eigenvalue. The standard Gaussian-3 (G3) compound method[21] was employed to determine final energies for all local minima. For transition states, the elements of the G3 method were used, viz. optimization to TS at HF/6-31G(d), frequencies at HF/6-31G(d), optimization to TS at MP2=full/6-31G(d), followed by four single-point energy determinations at the MP2=full/6-31G(d) geometry, viz. QCISD(T)/6-31G(d), MP4/6-31+G(d), MP4/6-31G(2df,p), and MP2=full/G3large, and the values were combined according to the G3 procedure.[21] The identities of the transition-state structures were verified by calculation of intrinsic reaction coordinates[22] at the MP2=Full/6-31G(d) or B3LYP/6-31G(d) levels. Reaction barriers were calculated as differences in G3 enthalpies at 298.15 K (quoted simply as ΔH in the tables and figures of results). Where required, harmonic frequencies were obtained from the values calculated at the HF/6-31G(d) level adjusted by the correction factor 0.893 appropriate to this level.[23]

Results

General Considerations. For each reaction of interest, it was independently verified during preliminary experiments that in a given reaction mixture, k_{obs} values were not dependent on the exciplex laser energy (50−70 mJ/pulse, routine variation) or the number of photolysis shots. Because static gas mixtures were used, tests with up to 15 shots were carried out. The constancy of k_{obs} (five shot averages) showed no effective depletion of reactants in any of the systems. The sensitivities of detection of both SiH_2 and SiD_2 were high but decreased with increasing temperature. Therefore, increasing quantities of precursor were required at higher temperatures. However, at any given temperature, precursor pressures were kept fixed to ensure a constant (but always small) contribution to k_{obs} values.

Kinetics of $SiD_2 + C_2H_2$, Reaction (D1). This reaction was investigated at five temperatures in the range 297−600 K. At each temperature and at 10 Torr total pressure (SF_6 bath gas), at least five runs at different partial pressures of C_2H_2 were carried out. The results of these runs are shown in Figure 1, which demonstrates the linear dependence of k_{obs} on $[C_2H_2]$, as expected for second-order kinetics. The second-order rate constants at 10 Torr, obtained by least-squares fitting to these plots, are shown in Table 1. The error limits are single standard deviations. Table 1 also includes the second-order rate constants obtained earlier[5] for reactions (H) and (D2). The general decrease of the intercept values of Figure 1 with increasing temperature indicates that the reaction of SiD_2 with $PhSiD_3$ has

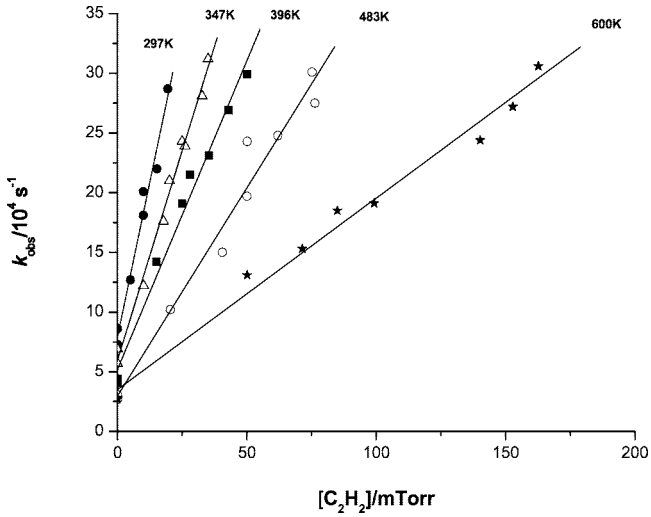

Figure 1. Second-order plots for reaction (D1), $SiD_2 + C_2H_2$, at 10 Torr (SF_6) at five temperatures (indicated).

TABLE 1: Experimental Second-Order Rate Constants[a,b] for SiD_2+ C_2H_2 and Analogous Reactions[c] Obtained at 10 Torr Total Pressure over the Range 291−613 K

T/K	$SiD_2 + C_2H_2$	*T*/K	$SiH_2 + C_2D_2$	*T*/K	$SiH_2 + C_2H_2$
297	3.18 ± 0.21	291	3.74 ± 0.16	291	3.21 ± 0.33
347	2.52 ± 0.08	346	2.94 ± 0.07	346	2.56 ± 0.04
396	2.12 ± 0.11	395	2.63 ± 0.06	399	1.99 ± 0.05
483	1.74 ± 0.12	481	2.02 ± 0.08	483	1.26 ± 0.04
600	1.00 ± 0.04	613	1.44 ± 0.06	613	0.61 ± 0.05

[a] Units: 10^{-10} cm^3 molecule^{-1} s^{-1}. [b] Single standard deviations. [c] Reference 5.

a negative activation energy. This is similar to the situation for $SiH_2 + PhSiH_3$[24] and was not pursued further.

In addition to these experiments, another set of runs was carried out at each temperature. In these runs, the total pressure (SF_6) was varied in the range 1−100 Torr, in order to test the pressure dependence of the second-order rate constants. The data were obtained in the same way as those at 10 Torr, although because second-order behavior had been established at 10 Torr, only three or four C_2H_2 partial pressures were tried at each total pressure. The rate constant for reaction of SiD_2 with precursor (intercept point on the second-order plots) was found to be pressure independent, similar to the reaction of SiH_2 with $PhSiH_3$.[24] The pressure range was limited by practical considerations. Above ca. 100 Torr, transient signals became too small, and below 1 Torr, pressure measurement uncertainties became significant. The results from these experiments are plotted in Figure 2, which clearly demonstrates the pressure dependence of the rate constants at each temperature. For convenience, log−log plots are used. The uncertainties are not shown in the figures, but they are estimated at ca. ±10%. These pressure dependencies show the rate constants converging toward a high-pressure limit at each temperature and showing an increasing degree of falloff as temperature increases, both characteristics of a third-body assisted association reaction. Nevertheless, the falloff effect is not large, and this enables us to estimate with reasonable confidence the high-pressure limiting values for the rate constants by extrapolation. These are shown in Table 2 along with those obtained earlier[5] for the analogous reactions of $SiH_2 + C_2D_2$ and $SiH_2 + C_2H_2$. Figure 3 shows an Arrhenius plot of the values obtained here for $SiD_2 + C_2H_2$ as well the rate constants at 10 Torr total pressure for comparison. The

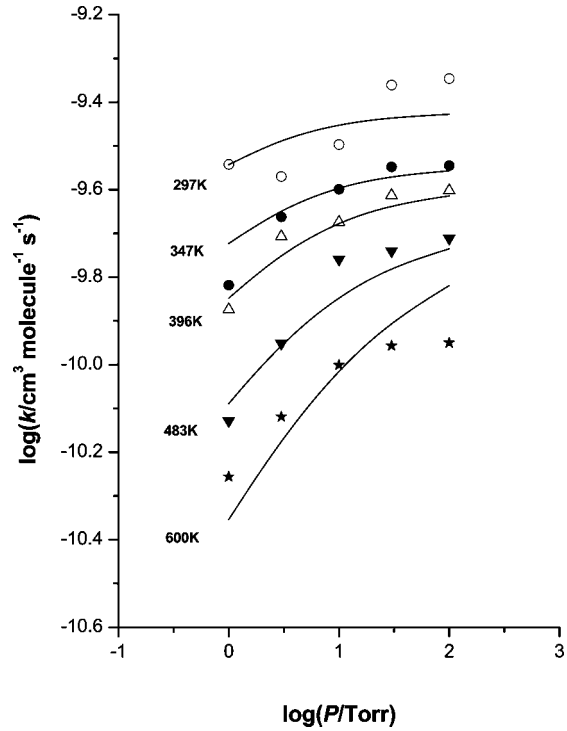

Figure 2. Pressure dependence of second-order rate constants for reaction (D1), $SiD_2 + C_2H_2$, in the presence of SF_6 at five temperatures (indicated). Curves are RRKM fits (see text).

TABLE 2: High-Pressure Limiting Second-Order Rate Constants[a,b] for SiD_2+ C_2H_2 and Analogous Reactions[c] Obtained over the Range 291−613 K

T/K	$SiD_2 + C_2H_2$	*T*/K	$SiH_2 + C_2H_2/C_2D_2$
297	3.76 ± 0.38	291	3.98 ± 0.40
347	2.82 ± 0.28	346	3.31 ± 0.32
396	2.51 ± 0.25	395	2.82 ± 0.28
483	2.00 ± 0.20	481	2.24 ± 0.22
600	1.88 ± 0.33	613	2.00 ± 0.25

[a] Units: 10^{-10} cm^3 molecule^{-1} s^{-1}. [b] Single standard deviations. [c] $SiH_2 + C_2H_2$ and $SiH_2 + C_2D_2$ found to have the same values within uncertainty limits (ref 5).

linear least-squares fit to the infinite pressure values corresponds to the Arrhenius equation:

$$\log(k^{\infty}/\text{cm}^3\ \text{molecule}^{-1}\ \text{s}^{1-}) = (-10.05 \pm 0.05) + (3.43 \pm 0.36)\ \text{kJ mol}^{-1}/RT \ln 10$$

Also shown in Figure 3 is the previously obtained Arrhenius line for $SiH_2 + C_2H_2/C_2D_2$.

Kinetics of SiH_2+ C_2H_2, Reaction (H). This reaction was investigated at three temperatures in the range 300−613 K. At each temperature and at 10 Torr total pressure (He bath gas), at least four runs at different partial pressures of C_2H_2 were carried out. The results of these runs are shown in Figure 4, which demonstrates the linear dependence of k_{obs} on [C_2H_2], as expected for second-order kinetics. The second-order rate constants at 10 Torr, obtained by least-squares fitting to these plots, are shown in Table 3. The error limits are single standard deviations. Table 3 also includes the second-order rate constants obtained earlier[5] for this reaction in the presence of SF_6. It is quite clear that the rate constants in the presence of He are less than those in SF_6 as might be expected for a less efficient collision partner.

The pressure dependence of the rate constants in this reaction was also investigated. At each temperature, the total pressure

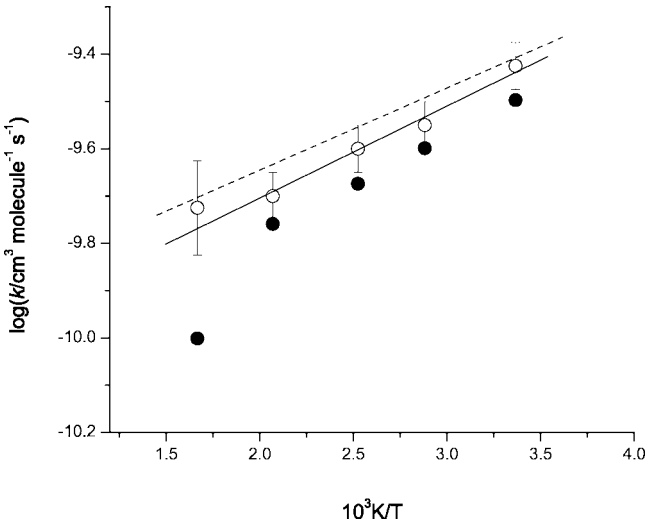

Figure 3. Arrhenius plots of second-order rate constants for reaction (D1), $SiD_2 + C_2H_2$ in SF_6. ●, 10 Torr; ○, k^∞. Solid line, reaction (D1); dashed line, reactions (H, D2).

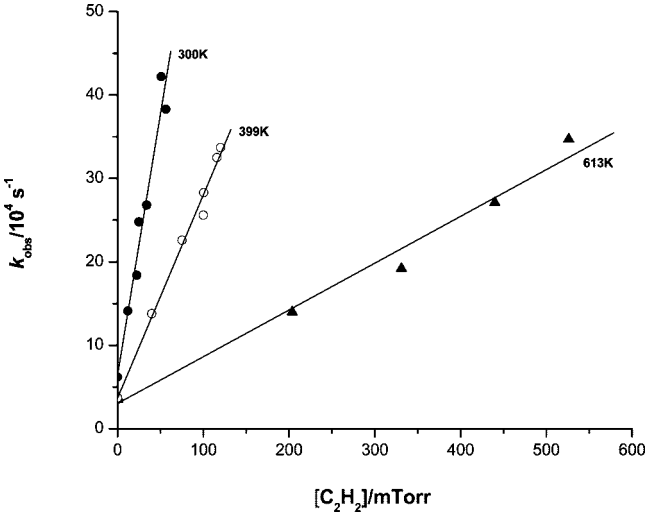

Figure 4. Second-order plots for reaction (H), $SiH_2 + C_2H_2$, at 10 Torr (He) at three temperatures (indicated).

TABLE 3: Experimental Second-Order Rate Constants[a,b] for $SiH_2 + C_2H_2$ Obtained at 10 Torr in He Compared with Those[c] Obtained in SF_6

T/K	*k* in He	*T*/K	*k* in SF_6
300	1.95 ± 0.14	291	3.21 ± 0.33
399	1.006 ± 0.035	399	1.99 ± 0.05
613	0.356 ± 0.022	613	0.61 ± 0.05

[a] Units: 10^{-10} cm^3 $molecule^{-1}$ s^{-1}. [b] Single standard deviations. [c] Reference 5.

(He) was varied by selecting five values in the range 1−100 Torr. Runs were carried out in the same way as those at 10 Torr, although because second-order behavior had been established at 10 Torr, only three or four C_2H_2 partial pressures were tried at each total pressure. The rate constant for reaction of SiH_2 with precursor (intercept point on the second-order plots) was found to be pressure independent.[24] The results from these experiments are plotted in Figure 5, which clearly demonstrates the pressure dependence of the rate constants at each temperature. For convenience, log−log plots are used. The uncertainties are not shown, but they are again estimated at ca. ±10%. These pressure dependencies show the same characteristics as those

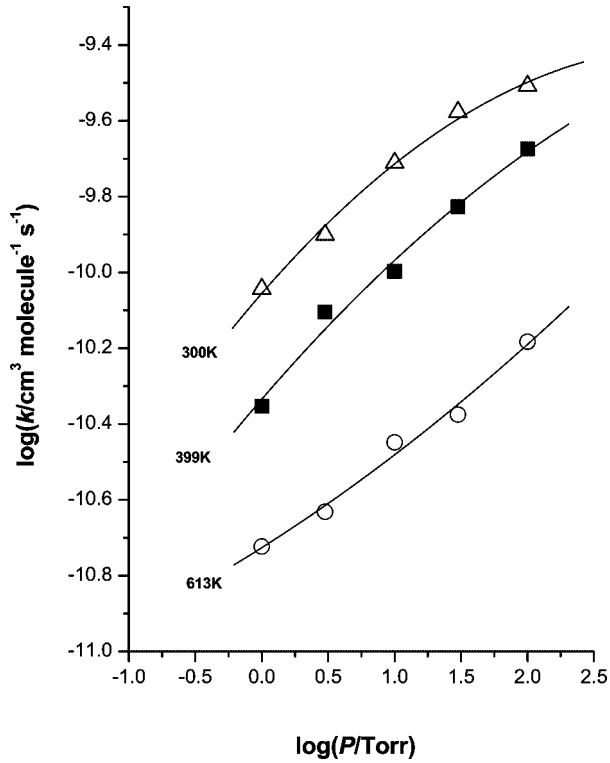

Figure 5. Pressure dependence of second-order rate constants for reaction (H), $SiH_2 + C_2H_2$, in the presence of He at three temperatures (indicated). Curves are eyeball fits.

TABLE 4: Kinetic Isotope Effects for Reactions $SiD_2 + C_2H_2$ (D1), $SiH_2 + C_2D_2$ (D2), and $SiH_2 + C_2H_2$ (H) in 10 Torr (SF_6) at Five Temperatures

T/K	k_{D1}/k_H	k_{D2}/k_H	k_{D1}/k_{D2}
294[a]	0.99 ± 0.12	1.165 ± 0.13	0.85 ± 0.07
346[a]	0.98 ± 0.03	1.15 ± 0.03	0.86 ± 0.03
397[a]	1.065 ± 0.06	1.32 ± 0.04	0.81 ± 0.05
483[a]	1.38 ± 0.10	1.60 ± 0.08	0.86 ± 0.07
613[b]	1.61 ± 0.15	2.36 ± 0.22	0.68 ± 0.04

[a] Average temperature of three systems. [b] k_{D1} values adjusted from 600 to 613 K.

of Figure 2. In this case, the extent of falloff is greater at a given pressure and temperature than that for reaction (D1) in SF_6. It is also larger than that for reaction (H) in SF_6 obtained earlier.[5] Comparisons of these data with RRKM theory are shown later (Figure 10). The lines shown in Figure 5 are simply eyeball fits.

Isotope Effects. Comparison of the rate constants of the present study with those of earlier work[5] permits the evaluation of several kinds of isotope effects. These are given here in order to provide the basis for comparison with theory and also the later discussion. Table 4 shows the isotope effects at 10 Torr (SF_6) as a function of temperature obtained by comparison of the rate constants (Table 1) of the three reaction systems, (D1), (D2), and (H). Where temperatures are a few degrees apart, they were averaged. Table 5 shows the isotope effects, k_{D1}/k_H, as a function of pressure (SF_6) and temperature obtained by comparison of the two systems, (D1) and (H). The rate constants on which the latter are based are included in the Supporting Information. Rate constants at 600 K (reaction D1) were reduced by 2% to correspond to 613 K. No corrections were made at other temperatures.

Quantum Chemical (Ab Initio) Calculations. Apart from the reactant species, $SiH_2 + C_2H_2$, 16 other minima and 15

TABLE 5: Kinetic Isotope Effects, k_{D1}/k_H, for Reactions $SiD_2 + C_2H_2$ (D1) and $SiH_2 + C_2H_2$ (H) as a Function of Pressure and Temperature[a]

	T/K				
P/Torr	294	346	397	483	613
100	1.30 ± 0.15	0.97 ± 0.12	0.95 ± 0.10	1.09 ± 0.11	1.00 ± 0.18
30	1.32 ± 0.40	1.03 ± 0.11	1.06 ± 0.13	1.17 ± 0.12	1.16 ± 0.14
10	1.05 ± 0.13	1.05 ± 0.11	1.11 ± 0.09	1.38 ± 0.17	1.45 ± 0.12
3	1.05 ± 0.12	1.25 ± 0.14	1.39 ± 0.11	1.20 ± 0.28	1.67 ± 0.15
1	1.58 ± 0.18	1.15 ± 0.14	1.40 ± 0.19	1.42 ± 0.24	2.73 ± 0.47

[a] Temperatures are averages of the original studies.

transition states (TS0, TS1, TS1a, TS1b, TS2, TS2a, TS2b, TS3−TS10) were found in these calculations. The minima correspond to a hydrogen-bonded complex (HC≡CH···SiH_2), silirene (c-H_2SiCH=CH−), 3-silapropenylidene (H_3SiCH=C), ethynylsilane (HC≡$CSiH_3$), vinylsilylene (H_2C=CHSiH) in both cis and trans forms, isosilirene (c-H_2CCH=SiH−), 1-silaallene (H_2C=C=SiH_2), 1-silapropenylidene (MeCH=Si), 1-silapropyne (MeC≡SiH), 2-silapropyne (MeSi≡CH), 1-siliranylidene (c-CH_2CH_2Si−), 2-silaallene (H_2C=Si=CH_2), 1-silirenylidene + hydrogen (c-CH=CHSi− + H_2) all in singlet (S) states, and C_2H_4 + Si in both S and T states. The minima and transition states TS1, TS1a, TS1b, and TS2−TS10 linking these species are shown on the PES in Figure 6. The additional transition states, TS0 (linking SiH_2 + C_2H_2 and ethynylsilane), TS2a (linking silirene and 1-silaallene) and TS2b (linking silirene and 1-silirenylidene + H_2) are omitted to keep complexity to a minimum and because their enthalpies are positive (see Discussion). Total enthalpies (at 298 K) and enthalpy values for all structures relative to the SiH_2 + C_2H_2 pair are listed in Table 6. The structures of the minima involved in these relatively low-energy pathways and the transition states are shown in Figures 7 and 8, respectively.

The G3 calculations were attempted on all plausible species, and G3Q calculations were only carried out where difficulties were encountered with structures calculated at the MP2=Full/6-31G(d) level. These are described below, where appropriate. In what follows, the enthalpies are G3 values unless otherwise stated. The most stable species on this surface is ethynylsilane ($\Delta H = -261$ kJ mol^{-1}), with silirene ($\Delta H = -218$ kJ mol^{-1}) next and fairly close to it in enthalpy. After that, the next four most stable species are all silylenes, 1-siliranylidene ($\Delta H = -203$ kJ mol^{-1}), 1-silapropenylidene ($\Delta H = -192$ kJ mol^{-1}), and *cis*- and *trans*-vinylsilylene ($\Delta H = -183$ and -186 kJ mol^{-1}, respectively). This attests to the long-known special stability of the silylenes.[25]

The large number of species and transition states indicates that there is considerable potential complexity in the reaction mechanism of SiH_2 with C_2H_2. In Figure 6, we have concentrated on presenting those species and pathways which are most likely to be involved in the reaction. Apart from TS0, TS2a, TS2b, and Si (both S and T states) + C_2H_4, all the remaining species and transition states lie below the reactant enthalpy. Thus, all species shown are energetically accessible, except Si + C_2H_4 and silirenylidene + H_2. This latter, although lower in enthalpy than SiH_2 + C_2H_2, is inaccessible because it can only be reached via TS2b which is highly positive in enthalpy. TS0 links SiH_2 + C_2H_2 directly with ethynylsilane (C−H insertion process), but the latter can be reached via the alternative, low-enthalpy pathway of silirene, TS1, 3-silapropenylidene, TS1a, or TS1b. TS2a links silirene and 1-silaallene, but the latter can be reached via the alternative, low-enthalpy pathway of TS2, vinylsilylene, and TS4. Among the accessible species (local minima), two groups may be distinguished. The first of these is the group of the most stable and comprises silirene, ethynylsilane, vinylsilylene (both *cis*- and *trans*-), 1-silaallene, 1-silapropenylidene, and 1-siliranylidene, all existing within relatively deep energy wells. The second group contains the less stable species, isosilirene, 1-silapropyne, 2-silapropyne, and 2-silaallene. These species each have low barriers leading to one member only of the more stable group: they offer no through routes to final products and may be described by the term shelf species, that is, species which lead nowhere but can exist temporarily on a high shelf if there is enough energy to reach it.[15] 3-Silapropenylidene is a unique species, because although it is relatively high in enthalpy, it appears to be a necessary intermediate in the formation of ethynylsilane.

According to the calculations, the initial reaction of SiH_2 with C_2H_2 results in the formation of silirene (Figure 6). No intervening π-complex could be discerned. The formation of a very weakly bound H-bonded complex (planar σ-type)[26] seems to lead nowhere, although we did not test whether it was a necessary intermediate in the Si−H insertion process (via TS0). Silirene can rearrange to both ethynylsilane and vinylsilylene via relatively low-energy pathways. [We do not draw a distinction between formation of *cis*- or *trans*-vinylsilylene nor their subsequent reactive behavior (see below).] It should be noted that vinylsilylene is formed endothermically, whereas ethynylsilane is formed exothermically. This means that although TS2 is lower in enthalpy than TS1, formation of vinylsilylene is highly reversible, and reaction via TS1 to ethynylsilane is likely to be more effective overall. The structures of TS1 and TS2 show that the mechanisms of rearrangement of silirene to ethynylsilane and vinylsilylene both involve rate-determining H-shift processes synchronous with ring-opening. The 1,2 H-shift from Si to C (TS2) directly results in vinylsilylene, but the 1,2 H-shift from C to Si (TS1) should produce 3-silapropenylidene. However, at the MP2=full/6-31G(d) level (and also the B3LYP/6-31G(d) level) searches for a stable minimum for this species only produced ethynylsilane. Only at QCISD=full/6-31G(d) could a stable species be found. Even so, 3-silapropenylidene rearranges with very low barriers to ethynylsilane via a 1,2-shift either involving an H atom (TS1a) or an SiH_3 group (TS1b). TS1b lies lower in enthalpy and could only be found at the QCISD level.

There are four accessible routes for further rearrangement of vinylsilylene, via transition states TS3−TS6. TS3 and TS6 are the two lowest enthalpy transition states and lie very close in value. TS3 involves a 1,3 H-shift from Si to C, to make 1-silapropenylidene. It is interesting to note that 1-silapropenylidene with its C=Si double bond is actually more stable than vinylsilylene, with a C=C double bond. TS6 requires a 1,2 H-shift from Si to C with simultaneous ring closure to make 1-siliranylidene. It is clear that both 1-silapropenylidene and 1-siliranylidene can be readily formed from SiH_2 + C_2H_2; moreover, because TS3 and TS6 are lower in enthalpy than TS2, it is almost certain that if vinylsilylene can be formed, these two silylenes will also be formed. However, it should be added that, just as vinylsilylene, they are endothermic with respect to silirene, and therefore, their formation will be highly reversible. TS4 involves a 1,2 H-shift from C to Si, but the product, 1-silaaallene, is again unstable with respect to silirene, and its formation will also be highly reversible. It is almost a shelf species. TS5 involves only a simple ring closure; however, the high enthalpy value arising largely from the strain of the resulting product, iso-silirene, with its internal C=Si double

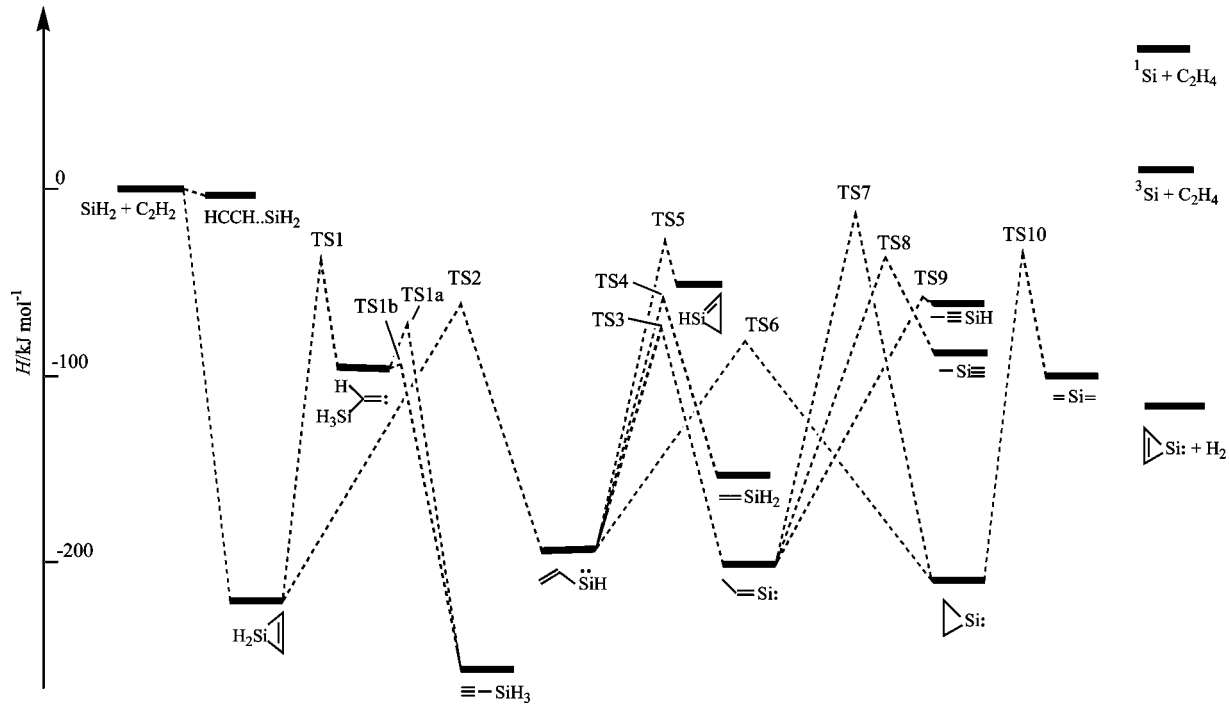

Figure 6. Potential energy (enthalpy) surface showing the SiC_2H_4 species most likely involved in the reaction of SiH_2 with C_2H_2. Enthalpy values calculated at the G3(G3Q) level.

TABLE 6: G3 and Selected G3Q Calculated Total Enthalpies, *H*/Hartree, and Relative Enthalpies, Δ*H*/kJ mol^{-1}, for Stationary Points of Interest on the SiC_2H_4 Energy Surface

species	G3[a] *H*(298 K)	ΔH_{rel}	G3Q[b] *H*(298 K)	ΔH_{rel}
$SiH_2 + C_2H_2$	−367.725970	0	−367.727046	0
HCCH···SiH_2 complex	−367.726772	−2		
silirene	−367.808909	−218	−367.810312	−219
3-silapropenylidene			−367.759626	−86
ethynylsilane	−367.825203	−261	−367.827203	−263
vinylsilylene(cis)	−367.795858	−183		
vinylsilylene(trans)	−367.796751	−186		
isosilirene	−367.747757	−57		
1-silaallene	−367.789509	−167		
1-silapropenylidene	−367.799060	−192	−367.799110	−189
1-silapropyne	−367.749575	−62	−367.756202	−77
2-silapropyne	−367.759000	−87		
1-siliranylidene	−367.703457	−203		
2-silaallene	−367.767510	−109		
1-silirenylidene + H_2	−367.775815	−131		
$^1Si + C_2H_4$	−367.695459	+80		
$^3Si + C_2H_4$	−367.723324	+7		
TS0	−367.710375	+41		
TS1	−367.741601	−41	−367.747150	−53
TS1a	−367.754500	−75	−367.753961	−71
TS1b			−367.762860	−94
TS2	−367.750552	−65	−367.753827	−70
TS2a	−367.694864	+82		
TS2b	−367.693740	+85		
TS3	−367.755851	−78		
TS4	−367.750903	−65		
TS5	−367.737710	−31		
TS6	−367.756470	−80		
TS7	−367.730098	−11		
TS8	−367.742706	−44		
TS9	−367.756926	−81	−367.756839	−78
TS10	−367.740943	−39		

[a] Full expression: G3//MP2=Full/6-31G(d). [b] Full expression: G3//QCISD/6-31G(d).

bond shows that this pathway is another dead end, and isosilirene is a shelf species.

Further reaction in this system would appear to be determined by the possible fates of 1-silapropenylidene and 1-siliranylidene. For the former of these two silylenes, two pathways to silapropynes were identified. The first via TS9, a 1,2 H-shift process, forms 1-silapropyne, and the second via TS8, a 1,2 Me-shift process, leads to 3-silapropyne. Both these species, high in enthalpy, have bent structures. Because, at G3, the enthalpy of TS9 lay significantly below that for 1-silapropyne itself, the structures were recalculated at the QCISD level, and the enthalpies were calculated at G3Q. The QCISD calculation showed that the distortion from linear is significantly dependent upon the level of calculation (e.g., at QCISD, the CSiH bond angle is 110.5° rather than the 147.2° found at MP2). The G3Q calculation gave enthalpy values for TS9 and 1-silapropyne much closer to each others, even though TS9 still lies below 1-silapropyne. This was not explored further because the relatively high enthalpy for 1-silapropyne means that it is clearly a shelf species regardless of the level of calculation. The same applies to 2-silapropyne, for which QCISD calculations were not carried out. Another pathway which links 1-silapropenylidene and 1-siliranylidene involves a synchronous ring closure and 1,2 H-shift via TS7. Although the enthalpy of TS7 lies below that of $SiH_2 + C_2H_2$, it is nevertheless high enough that any interconversion of these two species is much more likely to occur via TS3, vinylsilylene, and TS6. 1-Siliranylidene, the most stable silylene on the surface, appears to be the end of the line for important intermediates on this reaction surface. Although 1-siliranylidene can isomerize to 2-silaallene via a simple ring opening via TS10, the latter has no exit channel and is a shelf species.

By analogy with GeC_2H_4 surface,[15] the most likely fate of 1-siliranylidene would appear to be dissociation to $Si + C_2H_4$. Because the ground state of the silicon atom is $^3P_1$, this involves an intersystem crossing. Nevertheless, the enthalpy requirement is sufficient that the overall process from $SiH_2 + C_2H_2$ is endothermic (although only by 7 kJ mol^{-1}). Because this dissociation would seem to be ruled out on enthalpy grounds, we did not investigate the details of its possible mechanism. The spin conserved dissociation leading to Si ($^1D_2$) is even more endothermic.

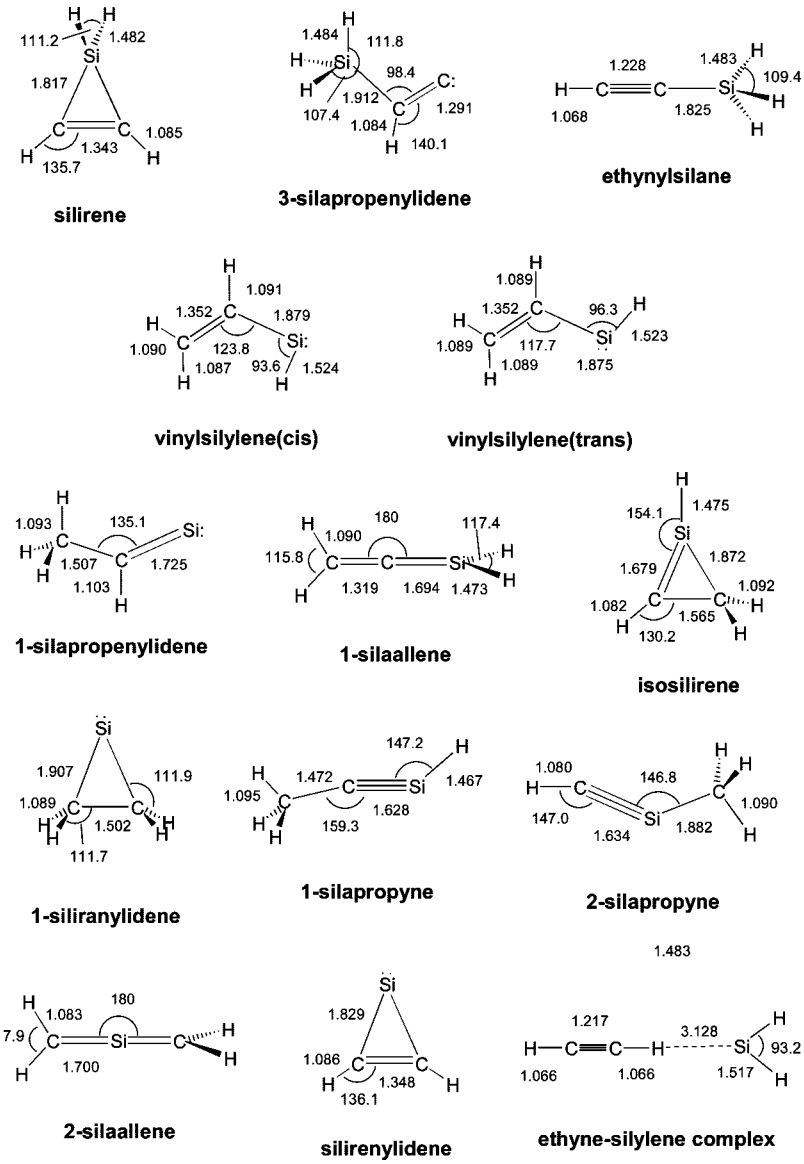

Figure 7. Ab initio, MP2=full/6-31G(d) calculated geometries of local minimum structures on the SiC_2H_4 surface. Selected distances are given in angstroms, and angles are given in degrees.

RRKM Calculations. The pressure dependence of an association reaction corresponds exactly to that of the reverse unimolecular dissociation process, providing there are no other perturbing channels.[27] The quantum chemical calculations in this reaction system have shown that there are other channels besides the simple addition reaction to form silirene. We have encountered this situation previously in several other systems.[15,28−33] Therefore, we adopted here an approach to modeling similar to that used earlier in the $GeH_2 + C_2H_2$ reaction.[15] It seems likely from the kinetics that the effective transition state (herein referred to as TSa) is that of the initial step (i.e., that to form silirene), whereas from the quantum chemical calculations, the end product is ethynylsilane. Thus, our procedure was first to construct a transition state appropriate to decomposition of silirene (to $SiH_2 + C_2H_2$) but then treat the reactant as if it were ethynylsilane (in rapid equilibrium with silirene). Thus, the process modeled by RRKM is essentially that shown in Scheme 2.

The RRKM calculations were carried out in combination with a collisional deactivation model (also called the master-equation method), details of which are given below. Because experimental details of the structures and vibrational wavenumbers of the species of interest here are not available, we have taken most of the necessary information from the output of the theoretical calculations.

SCHEME 2

$$HC{\equiv}CSiH_3 \underset{2}{\overset{-2}{\rightleftharpoons}} H_2Si{=}CH_2 \xrightarrow{-1} SiH_2 + C_2H_2$$

The vibrational assignment of the transition state (TSa) was obtained by the same procedure as previously,[5] based on adjustment of the vibrational wavenumbers for silirene to match the *A* factor for its decomposition (also evaluated previously). Variational character was introduced by calculating the *A* factor at each temperature of interest by using $\ln(A_{-1}/A_1) = \Delta S_{-1,1}^{\circ}/R$, where A_{-1} and A_1 are the decomposition and combination *A* factors, respectively, and $\Delta S_{-1,1}^{\circ}$ is the entropy change. The wavenumbers of the transitional modes were adjusted systematically in order to anticipate a similar exercise for the d_2-case (see below). The only difference here was to use the wavenumbers for silirene from the present calculations, which did not, however, differ significantly from results obtained previ-

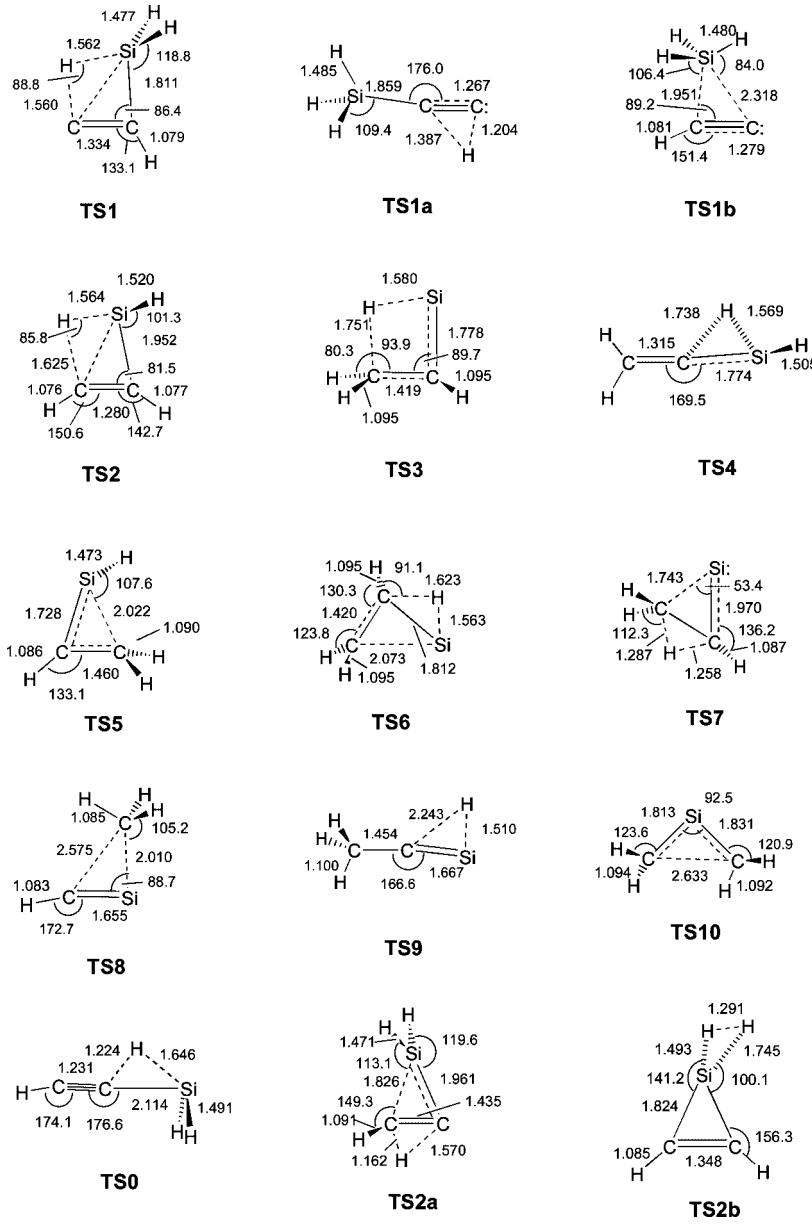

Figure 8. Ab initio, MP2=full/6-31G(d) calculated geometries of transition state structures on the SiC_2H_4 surface. Selected distances are given in angstroms, and angles are in degrees.

ously.[5] Likewise for the reactant molecule, ethynylsilane, the wavenumbers from the present calculations were used. The details of these for 613 K are given in Table 7. Details at other temperatures are given in the Supporting Information. The choice of E_o, the critical energy, is discussed below.

We have assumed, as previously,[15] that geometry changes between reactant and transition state do not lead to significant complications. In modeling the collisional deactivation process, we have used a weak collisional (stepladder) model,[27] because there is overwhelming evidence against the strong collision assumption.[34] The average energy removal parameters, $\langle\Delta E\rangle_{down}$, which determine the collision efficiencies, were taken as 12.0 kJ mol^{-1} (1000 cm^{-1}) for SF_6 (as used previously in this system)[5] and 1.8−3.0 kJ mol^{-1} (150−250 cm^{-1}) for He, by analogy with other systems.[34] In the helium-bath gas experiments, the effects of varying the dilution of the reactive species was briefly investigated. In these experiments, $\langle\Delta E\rangle_{down}$ for C_2H_2 was taken as 12.0 kJ mol^{-1} (1000 cm^{-1}).

In order to investigate the pressure dependence of the isotope effect, a similar exercise was carried out for the appropriate d_2 species. A number of effects of D-for-H substitution had to be taken into account. The vibrational wavenumbers of silirene-1,1-d_2 and ethynylsilane-1,1-d_2 were obtained from the theoretical calculations. Those for the transition state TSa(d_2) were obtained by adjustment of the vibrational wavenumbers of silirene-1,1-d_2 in the same systematic way as those for the nondeuterated case. Lennard-Jones collision numbers were adjusted for reduced mass effects (but nothing else). It was assumed that the energy removal parameters were not affected. Finally, the chosen E_o value (see below) was adjusted to take account of zero-point energy differences. Details of these parameters are given in the Supporting Information.

The results of these calculations are presented in Figures 9–11 and also in Figure 2. Figure 9 shows three calculations carried out for reaction (H) in the presence of SF_6 bath gas at 613 K. In curve A, it was assumed that the product was all stabilized as silirene, and E_o was taken as 203 kJ mol^{-1}, the value from the theoretical calculations. In curve B, the product was taken as ethynylsilane, and E_o = 246 kJ mol^{-1}, again the theoretical value, was used. In curve C, the product was ethynylsilane, and

TABLE 7: Molecular and Transition State Parameters for RRKM Calculations for Silirene and Ethynylsilane Decomposition at 613 K

	silirene	TSa	ethynylsilane
$\tilde{\nu}$/cm^{-1}	3043(1)	3043(1)	3262(1)
	3020(1)	3020(1)	2150(1)
	2141(1)	2141(1)	2143(2)
	2130(1)	2130(1)	2086(1)
	1483(1)	1483(1)	933(1)
	1133(1)	1133(1)	929(2)
	985(1)	985(1)	751(2)
	968(1)	968(1)	672(2)
	915(1)	915(1)	590(1)
	758(1)	694(1)	234(2)
	696(1)	91(1)	
	694(1)	89(1)	
	682(1)	77(1)	
	588(1)	72(1)	
	552(1)		
Reaction Coordinate/cm^{-1}	758		
Path Degeneracy	1		3
E_o(critical energy)/kJ mol^{-1}	203		267.8[a]
Collision Number (in SF_6) $Z_{LJ}/10^{-10}$ cm^3 molecule^{-1} s^{-1}	5.30		5.30
Collision Number (in He) $Z_{LJ}/10^{-10}$ cm^3 molecule^{-1} s^{-1}	6.67		6.67

[a] See text.

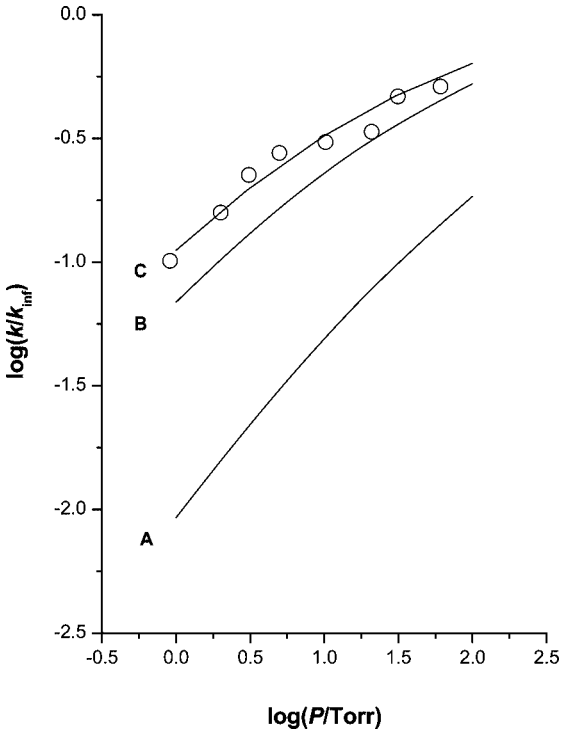

Figure 9. RRKM theoretical curves for pressure dependence of $SiH_2 + C_2H_2 \rightarrow H_3SiC{\equiv}CH$ at 613 K. Curves correspond to different critical energies (E_o/kJ mol^{-1}): **A**, 203; **B**, 246, **C**, 268. Experimental points: ○.

E_o was adjusted to a value of 268 kJ mol^{-1}, to provide the optimum fit. This graph shows that the simple association process alone cannot fit the data (results of ref 5). It also shows that stabilization of product as ethynylsilane, although providing a much closer correspondence to the experimental data, still does not fit well if we use the theoretical value for E_o. We therefore decided to use the optimum fit value for E_o for further

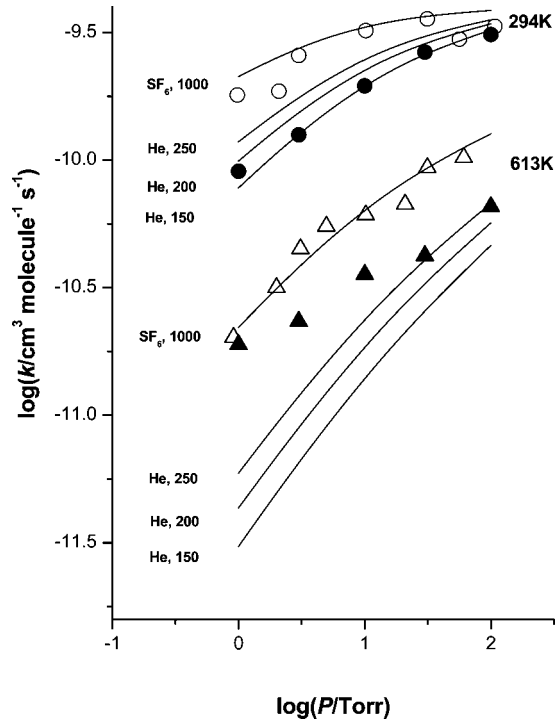

Figure 10. Comparison of RRKM theoretical curves with experiment for pressure dependence of $SiH_2 + C_2H_2 \rightarrow H_3SiC{\equiv}CH$ in both He (filled symbols) and SF_6 (open symbols) at two temperatures (indicated) and several different energy removal parameters ($<\Delta E>_{down}$/cm^{-1}).

calculations, while assuming the product was ethynylsilane. It should be mentioned that fitting (not shown) by using E_o = 268 kJ mol^{-1} at other temperatures of study to the original data[5] for reaction (H) was equally good as that at 613 K.

Figure 10 shows two sets of calculations for reaction (H) in the presence of He bath gas, at 294 and 613 K. At each temperature, the calculations employed values of 150, 200, and 250 cm^{-1} for $<\Delta E>_{down}$. For purposes of comparison, calculations for SF_6 bath gas are also shown, as well as the experimental data at both temperatures. Here, the fit at 294 K of the He bath gas data to $<\Delta E>_{down}$ = 150 cm^{-1} is good. At 613 K, the best fit, at the two highest pressures, corresponds to $<\Delta E>_{down}$ = 250 cm^{-1}, but the deviations become significant at lower pressure. Because some experimental runs at 613 K at 1 Torr involved use of up to 50% C_2H_2, some calculations were done with different dilutions of a strong collider (C_2H_2) in a weak collider (He). This had the effect of increasing calculated rate constants and therefore showed that at 1 Torr, part of the discrepancy with experiment could be due to this factor. At other total pressures, the dilutions were too great to have any significant effect. It should also be pointed out that such effects should give rise to curvatures in the second-order plots at low pressures. Within experimental error, this was not observed. Calculations at the third temperature of study, 399 K, were not included in Figure 10 to maintain clarity of presentation. The results are included in the Supporting Information, but they show a reasonable fit to the experimental data in He with a $<\Delta E>_{down}$ value between 200 and 250 cm^{-1}.

Figure 2 includes the results of the calculations for reaction (D1) with ethynylsilane-1,1-d_2 as product at each of the five temperatures of experimental study. The fits are reasonable within experimental scatter at the four lower temperatures. At 600 K, the RRKM-predicted trend of the rate constants with pressure is rather greater than that observed. Despite this, the calculated results for reactions (H) and (D1) were combined to

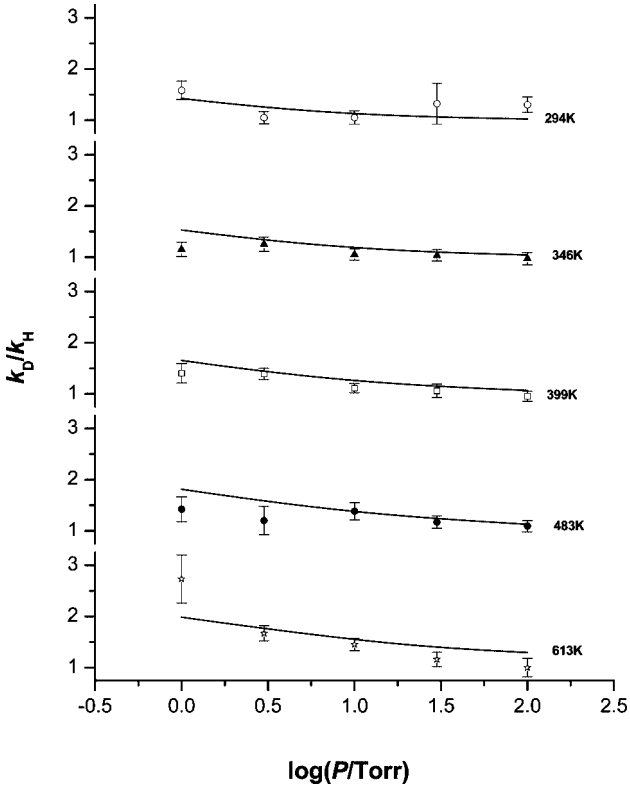

Figure 11. Comparison of RRKM calculated, pressure-dependent isotope effects, k_{D1}/k_H, with experiment at five different temperatures (indicated).

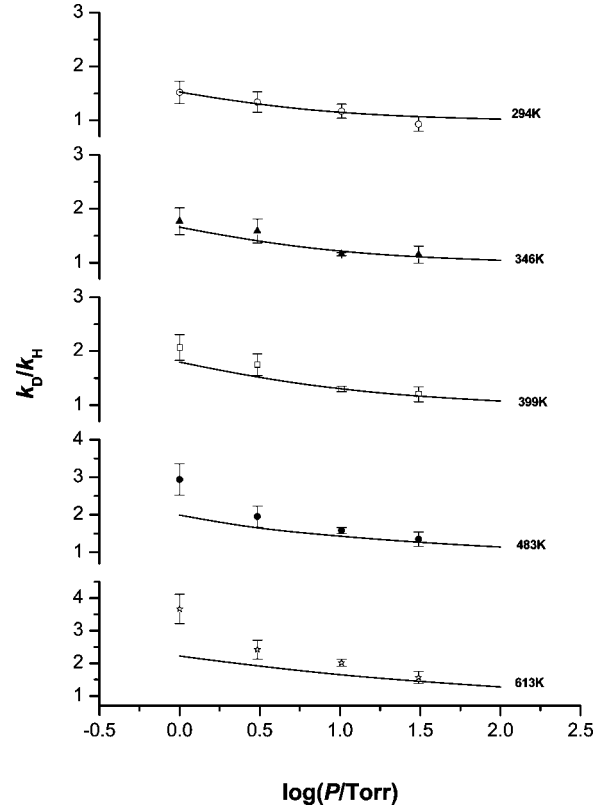

Figure 12. Comparison of RRKM-calculated-pressure-dependent isotope effects, k_{D2}/k_H, with experiment at five different temperatures (indicated).

obtain the RRKM-predicted-pressure-dependent inverse isotope effects, k_{D1}/k_H. These are compared with experiment in Figure 11. For purposes of simplification, it has been assumed that the high-pressure limiting ratio, $k_{D1}^{\infty}/k_H^{\infty}$, has the value of unity at all temperatures. The agreement between experiment and theory is satisfactory. The majority of calculated values are within the uncertainties of the experimental values. The theory shows that values of k_{D1}/k_H increase with increasing temperature and decreasing pressure, as observed.

Although not studied experimentally here, calculations of the isotope effect, k_{D2}/k_H, were carried out by using the same approach and assumptions as those for k_{D1}/k_H. In this case, the d_2 reactant species was ethynylsilane-1,3-d_2, and the TSa(d_2) corresponded to the loosened structure of silirene-2,3-d_2. Parameter details are given in the Supporting Information. The RRKM-calculated curves for $k_{D2}/k_H$are compared with experiment (data of ref 5) in Figure 12. It has again been assumed that the high-pressure limiting ratio, $k_{D2}^{\infty}/k_H^{\infty}$, has the value of unity at all temperatures. The agreement between experiment and theory is less satisfactory in this case and beyond the scatter in the data. Theory again shows that values of k_{D2}/k_H increase with decreasing pressure and increasing temperature, but the experimental trends are significantly more marked and show disagreement, especially at 483 and 613K at pressures below 10 Torr (SF_6).

Discussion

Kinetic Comparisons and the Nature of the Addition Process. The main experimental purpose of this study was to obtain new kinetic data to assist with the interpretation of the mechanism of the reaction of silylene with ethyne (acetylene). This has been accomplished in the form of a study of the pressure- and temperature-dependent kinetics of the reaction (D1) of SiD_2 with C_2H_2 in the presence of SF_6, together with a more limited study of the pressure and temperature-dependent kinetics of reaction (H) of $SiH_2 + C_2H_2$ in the presence of helium. There are no previous kinetic data on either of these specific reaction systems. The best comparisons are with the earlier study (by two of us[5]) of the kinetics of reactions (H) and (D2) of $SiH_2 + C_2D_2$ in the presence of SF_6. Table 1 shows that rate constants for reaction (D1) at 10 Torr (SF_6) are, within experimental error, the same as those for (H) at 294−397 K but greater at the two higher temperatures. On the other hand, under these conditions, rate constants for (D1) are less than those of (D2) at all temperatures. This is effectively shown in the isotope effects, k_{D1}/k_H and k_{D1}/k_{D2}, of Table 4. At the high-pressure limits, obtained by RRKM-assisted extrapolation, the rate constants for reaction (D1) differ slightly from those of reactions (H) and (D2), previously found to be the same, but are equal within experimental error. There is slightly greater uncertainty at the highest temperature (600 K) because of the poorer fit of theory to the pressure dependence (Figure 2). The Arrhenius plot (Figure 3) shows the close, although not identical, resemblance of the data obtained here for (D1) with that for (H) and (D2). The Arrhenius parameters are compared in Table 8 which also lists those for addition to alkenes.[35,36] There is no significant difference between the Arrhenius parameters for reaction (D1) and those for reaction (H) and (D2) and, indeed, the Arrhenius parameters for addition of SiH_2 to the alkenes. Although not shown, we have also found previously that the reactions of SiD_2 and SiH_2 with CH_3CHO,[37] another pressure-dependent association-reaction system, also had the same values for their high-pressure limiting rate constants and Arrhenius parameters.

The high collisional efficiencies for these addition reactions, calculated at ca. 64−82%,[38] show that they have very loose

TABLE 8: Arrhenius Parameters for Elementary Silylene Addition Reactions[a]

reaction	log(A/cm^3 molecule^{-1} s^{-1})	E_a/kJ mol^{-1}	ref
$SiD_2 + C_2H_2$	-10.05 ± 0.05	-3.4 ± 0.4	this work
$SiH_2 + C_2H_2(C_2D_2)$	-9.99 ± 0.03	-3.3 ± 0.2	5
$SiH_2 + C_2H_4$	-9.97 ± 0.03	-2.9 ± 0.2	35
$SiH_2 + C_3H_6$	-9.79 ± 0.05	-1.9 ± 0.3	36
$SiH_2 + i\text{-}C_4H_8$	-9.91 ± 0.04	-2.5 ± 0.3	36

[a] High-pressure limiting values.

TABLE 9: Comparison of Calculated Theoretical Energies (kJ mol^{-1}) for Stationary Points of Interest on the SiC_2H_4 Energy Surface[a,b]

species	Nguyen[c]	Maier[d]	Maier[e]	Skancke[f]	this work[g]
$SiH_2 + C_2H_2$	247			(250)	261
isosilirene		208			204
1-silapropyne					199
2-silapropyne					174
3-silapropenylidene				178 (162)	(177)
2-silaallene			140		152
1-silaallene		108	62	89 (74)	94
vinylsilylene(cis)		87	54		78
vinylsilylene(trans)	76	84	51	65 (54)	75
1-silapropenylidene		70	47		69
1-siliranylidene		62	48		58
silirene	48	50	38	62 (37)	43
ethynylsilane	0	0	0	0 (0)	0
TS1	172			224 (214)	220 (210)
TS1a				199 (190)	186 (192)
TS1b				169	(169)
TS2	154			197 (187)	196 (193)
TS4				197 (172)	196

[a] All energies include zpe. [b] Relative to ethynylsilane. [c] Reference 10, QCISD(TC)/6-311G++(2df,2p)/MP2/6−31G(d,p). [d] Reference 11, MP2/6-31G**. [e] Reference 12, BLYP/6-31G**. [f] Reference 13, CASP2//(12,12)CASSCF (B3LYP/6-31G*). [g] This work, G3 (G3Q).

transition states and, by implication, that any secondary reactions have very little influence on the rates at high pressures. It is not thought that intermediate complexes are involved; that is, the reactions are effectively concerted, although it is helpful to consider the addition process as involving two stages (electrophilic and nucleophilic). This has been discussed previously.[1−3,35,36]

The pressure dependence of reaction (H) in He, a weak collision partner, is expected to be more marked than that in SF_6, a strong collision partner, and this is indeed borne out by the comparison of rate constants in Table 3. The modeling of the pressure dependence of the rate constants (Figure 5) is shown in Figure 10 and is discussed later (see below).

Quantum Chemical Calculations and Mechanism. There have been several previous calculations[8−14] of parts of the SiC_2H_4 potential energy surface, although none as comprehensive as those of the present work. The results of the more recent, higher level of these calculations[10−13] are compared with ours in Table 9. The data of Raffy et al.[14] are not included because their results are not fully tabulated. For ease of comparison, the energy values are given relative to ethynylsilane, the universal minimum on the surface. The comparison is not quite strict because our numbers correspond to ΔH(298 K), whereas the others refer to ΔE(0K). However, the small effects of thermal energy should be largely canceling. The sequence of stabilities of the various stable species seems to be generally agreed. For the stable species, agreement between values is quite good where comparisons are possible. The values from the BLYP calculations[12] of Maier's group seem to be a little low. For transition states, the agreement between us and Skancke et al.[13] is particularly good, again where comparisons are possible. Our calculations agree with those of Nguyen et al.[10] and Skancke et al.[13] on the main features of the mechanism, as shown in Scheme 1. In the pathway to form ethynylsilane, the finding of a local minimum for 3-silapropenylidene depends on the level of calculation. Both Nguyen et al.[10] and Skancke et al.[13] report the failure to find it at the MP2/6-31G** level of theory, as did we. At higher levels of theory, our findings confirm those of Skancke et al.[13] that 3-silacyclopropenylidene prefers to rearrange via SiH_3- rather than H-migration.[39−41] Skancke et al.[13] also report that TS1b lies below the energy of 3-silapropenylidene, again similar to our results at G3Q. This supports the conclusion that 3-silapropenylidene is only very weakly (if at all) bound. There is also agreement with Nguyen et al.[10] and Skancke et al.[13] that the lowest-barrier pathway for silirene is to form vinylsilylene, but that this is endothermic. These features are also apparent in the potential energy surface shown by Raffy et al.[14] We also agree with Skancke et al.[13] that vinylsilylene can undergo further endothermic rearrangement to 1-silaallene. What our calculations have revealed, however, is that there is even greater complexity to this surface that hitherto indicated. Low-energy pathways from vinylsilylene to both 1-silapropenylidene and 1-siliranylidene have been found, indicating that these species will almost certainly be accessed starting from $SiH_2 + C_2H_2$, as well as from silirene itself. 1-Silapropenylidene and 1-siliranylidene are probably more likely intermediates than 1-silaallene in the deuterium scrambling mechanism of vinylsilylene-d_1 discovered by Maier et al.[11] The energetic accessibility of these species is also important in explaining the deuterium scrambling process proposed in our earlier studies of reaction (D2), $SiH_2 + C_2D_2$.[5] Although not clear to us at the time, there is a difficulty with our earlier proposal that H/D scrambling in silirene-2,3-d_2 occurs simply by involvement of vinylsilylene as an intermediate. This is illustrated in Scheme 3 below.

One of the constraints of this mechanism is that in the silirene ring-opening step, H-atom migration from Si to C can only result in the vinylsilylene with the H atom cis to the Si. In order for the silirene-2,3-d_2 to convert to silirene-1,2-d_2, the intermediate vinylsilylene-2,3-d_2 has to undergo cis/trans isomerization. Unassisted, this would require a high barrier and make the scrambling mechanism unviable. However, with the fairly low barriers associated with reversible mechanisms via 1-silapropenylidene and/or 1-siliranylidene (and/or 1-silaallene), this difficulty is removed. In these steps, H and D atoms become equivalent either by symmetry or by internal rotation of a CH_2D group.

Another point of significant interest is whether the species isosilirene plays any role in the overall mechanism of silirene or more specifically vinylsilylene rearrangements.[42,43] According

SCHEME 3

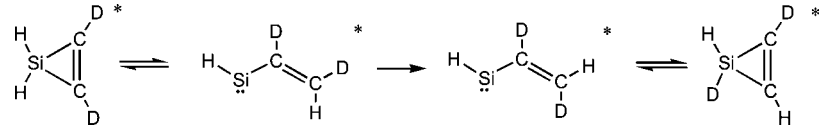

to our calculations, it seems that it is not the case. Although it is energetically accessible starting from $SiH_2 + C_2H_2$, there are three better (i.e., lower-energy) alternative pathways. Nevertheless, in the past, it was thought an attractive possibility because its formation from vinylsilylene can be viewed simply as an intramolecular π-addition of a silylene. Obviously because of the high energy of this pathway, this cannot be achieved. Nevertheless, the structures of the transition states for all of rearrangements of vinylsilylene (except TS4 to 1-silaallene) involve significant shortening of the 1,3 Si-to-C interatomic separation. From our calculations (see Figure 8), these Si-to-C distances (in angstroms) are the following: 2.022 (TS5), 2.073 (TS6), 2.170 (TS2), and 2.275 (TS3). The value in vinylsilylene is 2.775 Å. It can be argued that the three pathways via TS2, TS3, and TS6 represent attempts at ring closure by vinylsilylene foiled by H-migration steps which intervene as the Si-to-C separation diminishes and the strain increases. For substituted vinylsilylenes, Barton and co-workers[43] obtained evidence for 1-siliranylidene formation, that is, the pathway via TS6. Ethynylsilanes were also formed from vinylsilylenes in this[43] and earlier studies.[42] This essentially confirms the pathway via TS2, silirene, and TS1, although Barton did not rule out a mechanism via 1-silaallenes. Although we have not investigated the direct route from 1-silaallenes to ethynylsilanes via a direct 1,3 H-shift process, it was shown to be a high-energy pathway by Skancke et al.,[13] with an energy barrier of ca. 80 kJ mol^{-1} above that of TS1. This does rule it out.

One of the objectives of this work was to discover the likelihood of Si atom formation. The calculations show clearly that the reaction step

$$SiH_2 + C_2H_2 \rightarrow Si(^3P_1) + C_2H_4$$

is endothermic by 7 kJ mol^{-1}. This figure is in agreement with an estimate of 2.8 ± 8.3 kJ mol^{-1}, based on published ΔH_f^o values[25,44] for these species. Although the endothermic nature of this reaction makes it an unlikely competitor in the reaction of silylene with ethyne, nevertheless, the low value of ΔH^o means that a small contribution to the overall mechanism, at higher temperatures, could be a possibility. It is interesting to note that at ca. 700 K, Erwin et al.[45] found evidence for this reaction in a study of the pyrolysis of SiH_4 in the presence of C_2H_2. If this reaction occurs, the most likely route to $Si(^3P_1)$ formation would be via decomposition, with intersystem crossing, of 1-siliranylidene. Nevertheless, the differences between the potential energy surfaces for GeC_2H_4[15] and SiC_2H_4, revealed by these calculations do show why, in their respective reactions with C_2H_2, GeH_2, and SiH_2, they show different kinetic characteristics (pressure dependences).

RRKM Calculations and Further Mechanistic Comments. To a reasonable approximation, the RRKM calculations based on Scheme 2 provide a fit to the pressure- and temperature-dependent rate constants of reactions (H) and (D1). They also provide approximate fits to the pressure-dependent isotope effects, k_{D1}/k_H and k_{D2}/k_H. They get closer to experiment than the earlier modeling[5] based on silirene rather than ethynylsilane as the main product. However, when we look closely, there remain a number of difficulties. First, the E_o value required to fit is higher than that given by the quantum chemical calculations by ca. 22 kJ mol^{-1}. We doubt theory is in error by this much. Second. the pressure dependence in He at 613 K shows strong deviations from theory at low pressures (beyond those due to reduced dilution factors). Third, the experimental low-pressure values for k_{D1}/k_H and k_{D2}/k_H at 613 K show positive deviations from calculated values. The effects are all indicative of greater complexity in the mechanism than that of Scheme 2. The quantum chemical calculations discussed above support this. Although RRKM modeling on a multiwell potential energy surface is beyond the scope of this paper, it is clearly needed for further attempts to improve the fit in this reaction system. However, the basic pressure dependence of reaction (H) strongly suggests that ethynylsilane formation and stabilization is the major pathway. Other less stable products may provide temporary reservoirs for fractions of product formation but are all basically reversible with respect to silirene and ethynylsilane. The extent to which this may influence overall pressure dependence is not obvious. However, if a small fraction of the pathway produces $Si(^3P_1) + C_2H_4$, a non-pressure-dependent pathway, this will definitely reduce overall pressure dependence (at low pressures), thus having the same apparent effect which results in a higher than expected E_o value. A contribution of ca. 10% of this pathway would be sufficient to account for the deviation of the experimental points from theory in He at 613K (Figure 10). In relative terms, this would correspond to a free energy of activation difference of + 12 kJ mol^{-1} between this and the main pathway. Provided there is no special barrier or steric effect, this is sufficient to overcome the unfavorable endothermicity of +7 kJ mol^{-1}.

The lack of fit of the isotope effects (Figures 11 and 12) requires a different explanation. These can be accommodated by the low-barrier isomerization pathway to vinylsilylene, previously invoked[5] (see Scheme 1). The reversible nature of this step and the availability of further reversible isomerization pathways mean that D-for-H scrambling in the silirene can be achieved. This lowers the pressure dependence of the D-isotope reactions (D1) and (D2) as discussed previously.[1-3] The interesting finding in this work is that the isotope effects calculated are quite close to experiment for reaction (D1) under most conditions, although the deviations are more marked for reaction (D2). Thus, for reaction (D1), RRKM theory based on the simplified mechanism of Scheme 2 predicts isotope effects of the magnitude observed without an additional scrambling mechanism. For reaction (D2), this does not work. A possible explanation for this difference can be traced to the isotope-sensitive silirene isomerization steps as follows:

(D1)

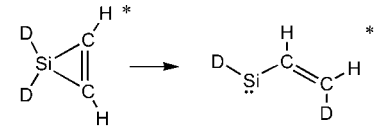

(D2)

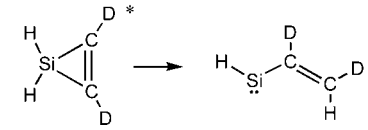

In reaction (D1), the ring opening is accompanied by a 1,2 D-atom shift, whereas in (D2), the process involves a 1,2 H-atom shift. In such processes, there is a primary isotope effect which will favor the H-migration process. Therefore, in the processes above, the step in (D2) should be faster than that in (D1). Because this is almost certainly the rate-controlling step for the isotopic scrambling process, this explains why reaction (D2) shows more evidence of scrambling, i.e., a bigger inverse isotope effect. A more complete (quantitative) explanation again requires further modeling which is beyond the scope of the present paper.

Conclusion

Kinetic studies of the reaction of $SiD_2 + C_2H_2$ are consistent with a pressure-dependent association mechanism to form initially silirene-1,1-d_2. The reaction has high-pressure limiting rate constants (and Arrhenius parameters) almost identical to those of $SiH_2 + C_2H_2$ and $SiH_2 + C_2D_2$ studied previously, but there is a pressure-dependent, inverse isotope effect (k_{D1}/k_H) which increases at low pressures and high temperatures. RRKM calculations show that this is more consistent with a mechanism in which the pressure dependence reflects the stabilization of vibrationally excited ethynylsilane (or ethynylsilane-d_2) rather than the initially formed silirene (or silirene-d_2). Nevertheless, the isotope effects (particularly k_{D2}/k_H) require the involvement of an isotope-scrambling process for silirene-1,1-d_2 (and silirene-2,3-d_2). Reversible isomerization of the silirene-d_2 to vinylsilylene-d_2 is the mechanism clearly indicated by ab initio calculations. The calculations also show the probable involvement of 1-silapropenylidene and 1-siliranylidene (and deuterated versions) in this isotope-scrambling mechanism, as well as rule out some other previously invoked pathways for the overall reaction. The slightly endothermic step

$$SiH_2 + C_2H_2 \rightarrow Si(^3P_1) + C_2H_4$$

could be a minor pathway (especially at temperatures >600 K) and would help explain the apparently low stabilizing efficiency of He bath gas in $SiH_2 + H_2$ studies at 613 K and the slightly high critical energy required for the modeling of the whole reaction.

Acknowledgment. R.B. thanks the Ministerio de Educacion y Ciencia for support under Project CTQ2006-10512/BQU. G.D. thanks the EPSRC for the award of a studentship.

Supporting Information Available: Experimental k_{D1} and k_H values as a function of pressure, experimental isotope effects, k_{D2}/k_H, comparison of experimental and RRKM-calculated pressure dependences for $SiH_2 + H_2 + He$ at 399 K, details of vibrational modes for silirene-1,1-d_2 and associated TSa, silirene-2,3-d_2 and associated TSa, ethynylsilane-1,1-d_2, and ethynylsilane-1,3-d_2, transitional vibrational modes for TSa for reactions (H), (D1), and (D2) at all temperatures, and full (unexpurgated) reference 20. This material is available free of charge via the Internet at http://pubs.acs.org.

References and Notes

(1) Jasinski, J. M.; Becerra, R.; Walsh, R. *Chem. Rev.* **1995**, *95*, 1203.
(2) Becerra, R. ; Walsh, R. Kinetics & mechanisms of silylene reactions: A prototype for gas-phase acid/base chemistry In *Research in Chemical Kinetics*; Compton, R. G., Hancock, G., Eds.; Elsevier: Amsterdam, 1995; Vol. 3, p 263.
(3) Becerra, R.; Walsh, R. *Phys. Chem. Chem. Phys.* **2007**, *9*, 2817.
(4) Gaspar, P. P.; West, R. Silylenes In *The Chemistry of Organic Silicon Compounds*; Rappoport, Z., Apeloig, Y., Eds.; Wiley: Chichester, 1998; Vol. 2, Chapter 43, p 2463.
(5) Becerra, R.; Walsh, R. *Int. J. Chem. Kinet.* **1994**, *26*, 45.
(6) Becerra, R.; Frey, H. M.; Mason, B. P.; Walsh, R. *Chem. Commun.* **1993**, 1050.
(7) Benson, S. W. *Thermochemical Kinetics*, 2nd ed.; Wiley: New York, 1976.
(8) Gordon, M. S.; Koob, R. D. *J. Am. Chem. Soc.* **1981**, *103*, 2939.
(9) Lien, M. H.; Hopkinson, A. C. *Chem. Phys. Lett.* **1981**, *80*, 114.
(10) Nguyen, M. T.; Sengupta, D.; Vanquickenborne, L. G. *Chem. Phys. Lett.* **1995**, *240*, 513.
(11) Maier, G.; Pacl, H.; Reisenauer, H. P. *Angew. Chem., Int. Ed. Engl.* **1995**, *34*, 1439.
(12) Maier, G.; Reisenauer, H. P.; Egenolf, H. *Eur. J. Org. Chem.* **1998**, 1313.
(13) Skancke, P. N.; Hrovat, D. A.; Borden, W. T. *J. Phys. Chem. A* **1999**, *103*, 4043.
(14) Raffy, C.; Allendorf, M. D.; Blanquet, E.; Melius, C. F. 15th Int. Symp. Chem. Vapor Deposition. *Proc. Electrochem. Soc.* **2000**, *13*, 40.
(15) Becerra, R.; Boganov, S. E.; Egorov, M. P.; Faustov, V. I.; Krylova, I. V.; Nefedov, O. M.; Promyslov, V. M.; Walsh, R. *Phys. Chem. Chem. Phys.* **2004**, *6*, 3370.
(16) Becerra, R.; Frey, H. M.; Mason, B. P.; Walsh, R.; Gordon, M. S. *J. Chem. Soc., Faraday Trans.* **1995**, *91*, 2723.
(17) Baggott, J. E.; Frey, H. M.; King, K. D.; Lightfoot, P. D.; Walsh, R.; Watts, I. M. *J. Phys. Chem.* **1988**, *92*, 4025.
(18) Jasinski, J. M.; Chu, J. O. *J. Chem. Phys.* **1988**, *88*, 1678.
(19) Mason, B. P.; Frey, H. M.; Walsh, R. *J. Chem. Soc., Faraday Trans.* **1993**, *89*, 4405.
(20) Frisch, M. J.; Trucks, G. W.; Schlegel, H. B.; Scuseria, G. E.; Robb, M. A.; Cheeseman, J. R.; Zakrzewski, V. G.; Montgomery, J. A., Jr.; Stratmann, R. E.; Burant, J. C.; Dapprich, S.; Millam, J. M.; Daniels, A. D.; Kudin, K. N.; Strain, M. C.; Farkas, O.; Tomasi, J.; Barone, V.; Cossi, M.; Cammi, R.; Mennucci, B.; Pomelli, C.; Adamo, C.; Clifford, S.; Ochterski, J.; Petersson, G. A.; Ayala, P. Y.; Cui, Q.; Morokuma, K.; Malick, D. K.; Rabuck, A. D.; Raghavachari, K.; Foresman, J. B.; Cioslowski, J.; Ortiz, J. V.; Stefanov, B. B.; Liu, G.; Liashenko, A.; Piskorz, P.; Komaromi, I.; Gomperts, R.; Martin, R. L.; Fox, D. J.; Keith, T.; Al-Laham, M. A.; Peng, C. Y.; Nanayakkara, A.; Gonzalez, C.; Challacombe, M.; Gill, P. M. W.; Johnson, B. G.; Chen, W.; Wong, M. W.; Andres, J. L.; Head-Gordon, M.; Replogle, E. S.; Pople, J. A. *Gaussian 98*, revision A.7; Gaussian, Inc.: Pittsburgh, PA, 1998.
(21) Curtiss, L. A.; Raghavachari, K.; Redfern, P. C.; Rassolov, V.; Pople, J. A. *J. Chem. Phys.* **1998**, *109*, 7764.
(22) Gonzales, C.; Schlegel, H. B. *J. Chem. Phys.* **1989**, *90*, 2154.
(23) Pople, J. A.; Scott, A. P.; Wong, M. W.; Radom, L. *Israel J. Chem.* **1993**, *33*, 345.
(24) The kinetics of the reaction of $SiH_2 + PhSiH_3$ have not been explicitly studied, but it is clear from our own many studies using $PhSiH_3$ as the SiH_2 precursor that the reaction rate constants have negative activation energies and are pressure independent. See, for example, ref 16.
(25) Becerra, R.; Walsh, R. Thermochemistry. In *The Chemistry of Organic Silicon Compounds*, Rappoport, Z., Apeloig, Y., Eds.; Wiley: Chichester, 1998; Vol. 2, Chapter 4, p 153.
(26) To our knowledge, this is the first calculated structure of a silylene complex in which the SiH_2 moeity is acting as a nucleophile.
(27) Holbrook, K. A.; Pilling, M. J.; Robertson, S. H. *Unimolecular Reactions*, 2nd ed.; Wiley; Chichester, 1996.
(28) Al-Rubaiey, N.; Becerra, R.; Walsh, R. *Phys. Chem. Chem. Phys.* **2002**, *4*, 5072.
(29) Becerra, R.; Boganov, S.; Egorov, M. P.; Faustov, V. I.; Krylova, I. V.; Nefedov, O. M.; Promyslov, V. M.; Walsh, R. *Phys. Chem. Chem. Phys.* **2002**, *4*, 5079.
(30) Becerra, R.; Walsh, R. *Phys. Chem. Chem. Phys.* **2002**, *4*, 6001.
(31) Becerra, R.; Cannady, J. P.; Walsh, R. *J. Phys. Chem. A* **2004**, *108*, 3987.
(32) Becerra, R.; Bowes, S-J.; Ogden, J. S.; Cannady, J. P.; Almond, M. J.; Walsh, R. *J. Phys. Chem.* **2005**, *109*, 1071.
(33) Becerra, R.; Cannady, J. P.; Walsh, R. *J. Phys. Chem. A* **2006**, *110*, 6680.
(34) Hippler, H.; Troe, J. In *Advances in Gas Phase Photochemistry and Kinetics*, Ashfold, M. N. R., Baggott, J. E., Eds.; Royal Society of Chemistry: London, 1989; Vol. 2, Chapter 5, p 209.
(35) Al-Rubaiey, N.; Walsh, R. *J. Phys. Chem.* **1994**, *98*, 5303.
(36) Al-Rubaiey, N.; Carpenter, I. W.; Walsh, R.; Becerra, R.; Gordon, M. S. *J. Phys. Chem. A* **1998**, *102*, 8564.
(37) Becerra, R.; Cannady, J. P.; Walsh, R. *Phys. Chem. Chem. Phys.* **2001**, *3*, 2343.
(38) Becerra, R.; Walsh, R. *J. Organomet. Chem.* **2001**, *636*, 49.
(39) The propensity for more rapid migration of the SiH_3 group than that of a H atom has been found previously in the thermal ring-opening reactions of various silyl-substituted cyclopropenes[40,41].
(40) Walsh, R.; Wolf, C.; Untiedt, S.; De Meijere, A. *J. Chem. Soc., Chem. Comm.* **1992**, 422.
(41) De Meijere, A.; Faber, D.; Heinecke, U.; Walsh, R.; Muller, T.; Apeloig, Y. *Eur. J. Org. Chem.* **2001**, 663.
(42) Barton, T. J.; Burns, G. T.; Goure, W. F.; Wulff, W. D. *J. Am. Chem. Soc.* **1982**, *104*, 1149.
(43) Barton, T. J.; Burns, G. T. *Tetrahedron Lett.* **1983**, *24*, 159.
(44) Chase, M. W., Jr. NIST-JANAF Thermochemical Tables 4th ed. *J. Phys. Chem. Ref. Data.*; 1998, Monograph 9.
(45) Erwin, J. W.; Ring, M. A.; O'Neal, H. E. *Int. J. Chem. Kinet* **1985**, *17*, 1067.

JP803391G